

Deadlock-Free Hybrid RL-MAPF Framework for Zero-Shot Multi-Robot Navigation

Haoyi Wang²

HAOYI@WUSTL.EDU

Licheng Luo¹

LICHENGL@UCR.EDU

Yiannis Kantaros²

IOANNISK@WUSTL.EDU

Bruno Sinopoli²

BSINOPOLI@WUSTL.EDU

Mingyu Cai¹

MINGYU.CAI@UCR.EDU

¹*Department of Mechanical Engineering, University of California Riverside, CA, USA*

²*Department of Electrical and Systems Engineering, Washington University in St. Louis, MO, USA*

Abstract

Multi-robot navigation in cluttered environments presents fundamental challenges in balancing reactive collision avoidance with long-range goal achievement. When navigating through narrow passages or confined spaces, deadlocks frequently emerge that prevent agents from reaching their destinations, particularly when Reinforcement Learning (RL) control policies encounter novel configurations out of learning distribution. Existing RL-based approaches suffer from limited generalization capability in unseen environments. We propose a hybrid framework that seamlessly integrates RL-based reactive navigation with on-demand Multi-Agent Path Finding (MAPF) to explicitly resolve topological deadlocks. Our approach integrates a safety layer that monitors agent progress to detect deadlocks and, when detected, triggers a coordination controller for affected agents. The framework constructs globally feasible trajectories via MAPF and regulates waypoint progression to reduce inter-agent conflicts during navigation. Extensive evaluation on dense multi-agent benchmarks shows that our method boosts task completion from marginal to near-universal success, markedly reducing deadlocks and collisions. When integrated with hierarchical task planning, it enables coordinated navigation for heterogeneous robots, demonstrating that coupling reactive RL navigation with selective MAPF intervention yields a robust, zero-shot performance. Additional details are available at <https://wanghaoyi518.github.io/rl-mapf-project-page/>.

Keywords: Reinforcement Learning, Multi-Agent Systems, Navigation, Motion planning

1. Introduction

Multi-agent long-range navigation in obstacle-rich environments requires both global guidance and reliable local interaction handling. Classical geometric local planners such as Velocity Obstacles (VO) / Reciprocal Velocity Obstacles (RVO) / Optimal Reciprocal Collision Avoidance (ORCA) offer fast, distributed collision avoidance (Fiorini and Shiller, 1998; Snape et al., 2011; van den Berg et al., 2011; Alonso-Mora et al., 2012), while deep RL controllers leverage high-dimensional observations for reactive goal pursuit and short-horizon interactions (Everett et al., 2018; Chen et al., 2017, 2019; Han et al., 2022). For long-range tasks, a common practice is to generate a coarse *global path* (e.g., A* or Theta*) and let the RL policy *track a sequence of waypoints* along that path, combining topological guidance with learned local navigation (Hart et al., 1968; Nash et al.,

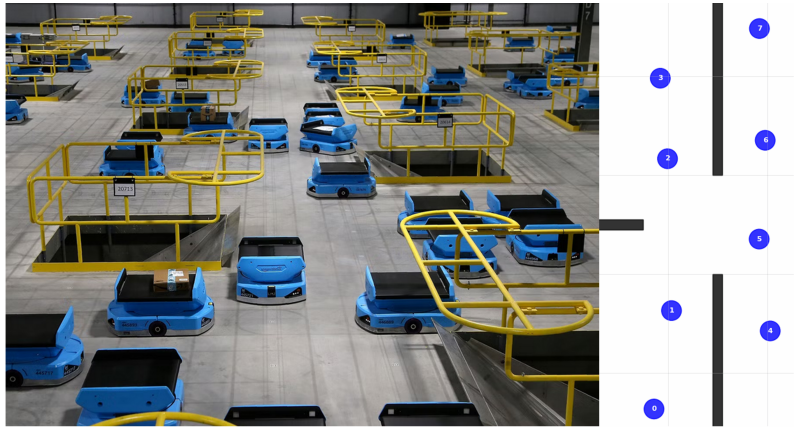


Figure 1: Deadlock phenomenon in practice and simulation. Reciprocal avoidance can saturate at bottlenecks, leading to deadlocks (photo adapted from [Bui \(2023\)](#)).

2007, 2010; [Yakovlev and Andreychuk, 2017](#); [Cai et al., 2023](#); [Luo and Cai, 2025](#)). This “global waypoints + local RL” pattern has been widely adopted to bridge large-scale routing with dynamics-aware local control. However, RL-based distributed navigation *alone* often struggles to generalize in complex, unseen layouts; the space of environmental patterns is vast, and purely learned policies can deteriorate out-of-distribution. Even under the waypoint-tracking setup, *multi-agent* deployments introduce additional failure modes: independently generated waypoint lists can place agents on *mutually proximate* targets or corridors, triggering persistent reciprocal avoidance that prevents agents from reaching waypoints. To define such mechanisms, We say a *deadlock* occurs (see Fig. 1) when a subset of agents, under purely reciprocal/local policies, enters a persistent standstill at a bottleneck and cannot make goal-directed progress ([Dergachev and Yakovlev, 2021](#); [Grover et al., 2019](#); [Wang and Botea, 2008](#)).

On the other hand, MAPF methods can compute coordinated, collision-free paths with near-optimality guarantees on discretized graphs ([Sharon et al., 2015](#); [Barer et al., 2014](#); [Li et al., 2021b](#); [de Wilde et al., 2014](#); [Surynek et al., 2021](#)), but incur non-trivial computational cost at scale and—crucially—typically assume agents can *faithfully follow* planned paths under simplified kinematic or time models, which may be brittle in practice; these issues motivate using global plans for guidance while avoiding always-on team-wide coordination ([Stern et al., 2019a](#); [van den Berg et al., 2011](#); [Ma et al., 2021](#); [Li et al., 2021c](#); [Ge et al., 2025](#); [Huang et al., 2024](#)).

We propose a *triggered hybrid* that preserves decentralized efficiency almost everywhere while injecting *locally confined coordination* only when necessary. By default, robots run an *RL mode* that tracks a global waypoint list and performs reciprocal avoidance. When a lightweight *deadlock detector* flags a persistent standstill around a bottleneck (e.g., a doorway swap), we crop a local grid over the implicated agents and solve a small MAPF instance. For each such agent, the solver returns a short *dense waypoint list*—a time-ordered sequence of reference waypoints. *Crucially, the low-level controller remains the same RL policy*, which now tracks these dense waypoints while handling local avoidance; non-implicated agents continue in the default RL mode. After the dense lists are executed (the stalemate cleared), agents seamlessly return to tracking their original global

waypoints. The local subplans rely on grid-based coordination primitives for quick, topology-aware disentanglement with bounded spatial/temporal scope (de Wilde et al., 2014; Barer et al., 2014; Li et al., 2021b).

The key is to *separate regimes by topology and time scale*. (i) In easy regimes with ample free space, reactive RL/ORCA-like behavior suffices for progress and safety (van den Berg et al., 2011; Alonso-Mora et al., 2012). (ii) In permutation-constrained regimes (doorways, swaps, narrow loops) where deadlocks are detected, a brief, *locally confined* MAPF solve produces for only the implicated agents a short *dense waypoint list* that is topologically valid for disentanglement (de Wilde et al., 2014; Sharon et al., 2015). Because the *low-level controller remains the same RL policy*, these dense waypoints act as short-horizon references while RL continues to handle reciprocal avoidance and dynamics; once executed, agents revert to tracking their original global waypoints. Thus coordination is *on demand and local*, keeping the amortized overhead small while reliably breaking stalemates by reordering a few agents rather than coordinating the whole team (Dergachev et al., 2020; Dergachev and Yakovlev, 2021; Stern et al., 2019a). The contributions are as follows: (i) A *deadlock-triggered, locally confined MAPF* module that augments a decentralized RL navigator only when needed; (ii) a practical pipeline that unifies reactive waypoint tracking with brief, topology-aware reordering, keeping computation and intervention *localized*; (iii) empirical evidence across dense exchanges and narrow passages showing high success, compared against strong baseline (Han et al., 2022). Additional materials can be found on the project website <https://wanghaoyi518.github.io/rl-mapf-project-page/>.

2. Related Work

RL-based multi-robot navigation. Deep reinforcement learning (DRL) has emerged as a powerful paradigm for interactive, decentralized collision avoidance, where a policy maps onboard observations of nearby agents/obstacles to continuous controls with no explicit communication. Early work such as CADRL/GA3C-CADRL learned value or policy networks that anticipate reciprocal interactions among multiple decision-making agents, later incorporating attention to model higher-order human–robot and human–human influences in dense crowds (Chen et al., 2017; Everett et al., 2018; Chen et al., 2019). Sensor-level DRL for multi-robot collision avoidance and crowd navigation further improves generalization across layouts and team sizes (Long et al., 2018; Fan et al., 2020). These approaches show strong short-horizon reactivity and scalability to a variable number of neighbors, but may suffer from myopic behaviors and limited long-range consistency, especially in cluttered layouts with bottlenecks and symmetry-induced stand-offs. Structure-aware formulations that encode velocity-obstacle geometry into the learning pipeline, e.g., using VO/RVO/ORCA vectors in the observation and shaping rewards with predicted collision time, improve safety and data efficiency while retaining decentralized execution (Fiorini and Shiller, 1998; van den Berg et al., 2011; Snape et al., 2011; Alonso-Mora et al., 2012; Han et al., 2022). Classical highly parallel local planners (e.g., ClearPath) underscore the efficiency of VO-style formulations but share the same deadlock risks under reciprocity (Guy et al., 2009). Our RL navigation policy follows this line by leveraging RVO-shaped state/reward design yet targets *long-range* settings where purely reactive reciprocity is insufficient.

MAPF and hybrid navigation. MAPF plans joint, collision-free trajectories on discrete abstractions. Optimal and bounded-suboptimal variants of Conflict-Based Search provide strong solution-quality guarantees, while complete polynomial-time schemes such as Push-and-Rotate ensure fea-

sibility under sufficient free space (Sharon et al., 2015; Barer et al., 2014; Li et al., 2021b; de Wilde et al., 2014; Boyarski et al., 2015). For geometric guidance over long distances, global planners like A* supply compact waypoint sequences. MAPF has continued to scale via anytime/meta-heuristics (MAPF-LNS) and analyses of solution-quality vs. team size (Li et al., 2021a; Atzmon et al., 2020), with extensions to continuous time important for bridging to execution (Andreychuk et al., 2022). Benchmarks and surveys consolidate definitions, variants, and standardized evaluation (e.g., MovingAI) (Stern et al., 2019a,b).

Purely reactive stacks (e.g., ORCA) are computationally efficient and provably collision-free under reciprocity assumptions but are prone to deadlocks in narrow passages; hybrid pipelines therefore combine global/any-angle waypoints with reciprocal avoidance during execution and *escalate* to locally confined MAPF when detectors flag prospective topological deadlocks (van den Berg et al., 2011; Dergachev et al., 2020; Dergachev and Yakovlev, 2021). Empirically, integrating Push-and-Rotate or (E)ECBS as an on-demand subsolver within an ORCA/Theta* stack boosts success dramatically in tight environments; we build on this architecture but replace hand-crafted local controllers with an RVO-shaped RL policy, preserving fast decentralized response while invoking MAPF only when necessary to re-order agents and restore flow (de Wilde et al., 2014; Barer et al., 2014; Li et al., 2021b; Dergachev et al., 2020; Dergachev and Yakovlev, 2021).

3. Problem Formulation

We consider a team of n circular agents $\mathcal{A} = \{1, \dots, n\}$ moving in a static two-dimensional workspace $W \subset \mathbb{R}^2$ that contains obstacles $O \subset W$ and free space $F = W \setminus O$. Each agent i has radius $r_i > 0$, state $x_i(t) = (p_i(t), v_i(t))$, position $p_i(t) \in F$, velocity $v_i(t) \in \mathbb{R}^2$, and speed limit $\|v_i(t)\| \leq v_i^{\max}$, where time is discrete with step size $\Delta t > 0$. Agents sense and communicate within a fixed range $R > 0$; the neighbor set of agent i at time t is defined as $\mathcal{N}_i(t) = \{j \in \mathcal{A} \setminus \{i\} \mid \|p_j(t) - p_i(t)\| \leq R\}$, and agents exchange only the local information necessary for reciprocal avoidance and deadlock resolution. Each agent i is assigned a start position $s_i \in F$ and a goal position $g_i \in F$, and the objective is to drive all agents from their respective start to goal positions.

A joint trajectory $\Pi = \{\pi_1, \dots, \pi_n\}$ with $\pi_i = \{p_i(t)\}_{t \geq 0}$ is considered collision-free if, for all t and all $i \neq j$, (i) $p_i(t) \in F$ and (ii) $\|p_i(t) - p_j(t)\| > r_i + r_j$; in practice, each agent selects instantaneous velocities that satisfy reciprocal collision-avoidance constraints with both neighbors and obstacles. A run is deemed successful if there exists a finite time T such that $p_i(T) = g_i$ for all i while maintaining safety for all $t \leq T$; the team success rate is reported in experiments. At each time step, each agent applies a decentralized hybrid control policy π_{RL} that uses local observations to generate a commanded velocity driving progress toward the goal while avoiding collisions with nearby agents and obstacles. When local progress stalls or reciprocal stand-offs occur, a deadlock is detected using the predicate:

$$\text{deadlock}(t) = \text{true} \quad \text{if} \quad \underbrace{\frac{1}{k} \sum_{\tau=t-k+1}^t \text{prog}_i(\tau) < \varepsilon_p}_{\text{ego progress}} \quad \wedge \quad \underbrace{\sum_{j \in \mathcal{N}_i(t)} \mathbf{1}\{\text{prog}_j^{(k)} < \varepsilon_p\} \geq \varepsilon_n}_{\text{neighbors stalled}}. \quad (1)$$

Detection of a deadlock triggers the formation of a locally confined MAPF instance over a grid subregion $G' \subset F$ encompassing the involved agents and relevant obstacles. The subproblem uses

the agents' current positions as starts and local waypoints as goals. A MAPF solver then computes a short-horizon joint plan for the affected agents, which they execute synchronously before returning to the decentralized policy π_{RL} . For long-range navigation, agents may optionally follow sparse guidance waypoints generated by a global planner on F (e.g., A*), serving as intermediate targets for π_{RL} between MAPF interventions.

Objective. Develop an integrated framework combining the decentralized policy π_{RL} , the deadlock predicate, subregion construction G' , and the MAPF solver \mathcal{P} to maximize team success in cluttered, previously unseen environments, while minimizing coordination overhead and maintaining the efficiency and responsiveness of π_{RL} during normal operation.

4. Methodology

We adopt the agent model, sensing assumptions, and VO/RVO formalism defined in Problem Formulation. Our controller is layered and switches *only* a small, locally selected group when necessary; all other agents remain in decentralized RL. *How the pieces connect:* §4.1 first produces per-agent *global waypoint lists* on a grid to provide long-range guidance. §4.2 details the *RL navigation policy* that runs at every step for all agents, encoding VO/RVO-based neighbor features and outputting smooth velocity increments that track either the global waypoints (default) or temporary dense waypoints. §4.3 monitors short-horizon progress and reciprocal interactions to *trigger* coordination only when local stalemates are detected. Upon a trigger, §4.4 forms a small *locally confined MAPF* on a cropped subgrid (PnR / bounded-suboptimal CBS variants) and returns, for the implicated agents only, a short *dense waypoint list*. These waypoints are executed by the *same* RL low-level policy; once completed, agents *seamlessly hand back* to the default RL navigation and continue tracking their original global waypoints. §4.5 gives formal verification for the mathematical properties of our method. The overall workflow is summarized in Fig. 2.

4.1. Global Path Planning (Waypoint Generation): Each agent i is assigned a long-range geometric *guide* Γ_i from start $p_{i,0}$ to goal g_i on a known static map. We adopt a grid-based shortest-path planner (e.g., A* (Hart et al., 1968)) at a resolution shared with local planning to avoid frame/scale drift and then *resample* the path into a waypoint sequence $\mathcal{W}_i = \{w_{i,k}\}_{k=0}^{K_i}$ (uniform or distance-threshold spacing). At runtime, the waypoint manager advances the active waypoint when within a reach threshold.

4.2. RL navigation policy: We use a decentralized learned local navigation policy that outputs smooth velocity *increments* and runs on-board for each agent. Agents are discs of radius R moving in $\mathcal{W}_{\text{free}}$ with step Δt ; the ego agent i has pose $p_{i,t} \in \mathbb{R}^2$ and velocity $v_{i,t} \in \mathbb{R}^2$, and we update

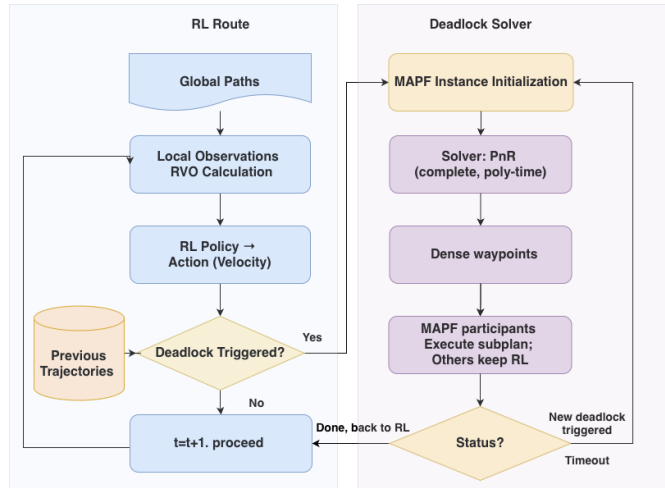


Figure 2: Hybrid RL+MAPF workflow.

$v_{i,t+1} = \text{clip}(v_{i,t} + \mu \Delta v_{i,t}, \|\cdot\| \leq v_{\max})$ and $p_{i,t+1} = p_{i,t} + v_{i,t+1} \Delta t$, where the policy outputs $\Delta v_{i,t}$ which is converted from (v_x, v_y) to (v, ω) by a heading-alignment controller.

Observations. We encode ego–neighbor information using VO/RVO geometry (Fiorini and Shiller, 1998; van den Berg et al., 2011; Han et al., 2022). Let $\text{ori}_{i,t} \in (-\pi, \pi]$ be heading, g_i the goal, w_i^{curr} the active global waypoint, and $v_{i,t}^{\text{des}} = k_p \frac{w_i^{\text{curr}} - p_{i,t}}{\|w_i^{\text{curr}} - p_{i,t}\|}$ with gain $k_p > 0$. Neighbors within radius R_{sense} form $\mathcal{N}_i(t) = \{j \neq i \mid \|p_{j,t} - p_{i,t}\| \leq R_{\text{sense}}\}$. For each $j \in \mathcal{N}_i(t)$, we build a 6D descriptor $c_{ij} = (v_{ij}^{\text{apex}}, \ell_{ij}^L, \ell_{ij}^R) \in \mathbb{R}^6$ with apex $v_{ij}^{\text{apex}} = v_{j,t}$ and VO boundary rays $\ell_{ij}^{L/R}$ induced by relative position $p_{j,t} - p_{i,t}$ and combined radius $R_c = 2R$; we also record distance $d_{ij} = \|p_{j,t} - p_{i,t}\|$. The time-to-collision $t_{ij}^{(e)}$ is the smallest $\tau > 0$ such that $v_{i,t} - v_{j,t} \in \text{VO}_{ij}(\tau)$ (set to $+\infty$ if no collision is predicted), and we map it to a scalar risk $r_{ij}^{(e)} = 1/(t_{ij}^{(e)} + 0.2)$ to emphasize imminence. The policy input is $o_{i,t}^{\text{self}} = [v_{i,t}, \text{ori}_{i,t}, v_{i,t}^{\text{des}}, R_c]$ and $o_{i,t}^{\text{sur}} = \{(c_{ij}, d_{ij}, r_{ij}^{(e)})\}_{j \in \mathcal{N}_i(t)}$.

Network & training. We aggregate the variable-size set $\{(c_{ij}, d_{ij}, r_{ij}^{(e)})\}$ with a BiGRU encoder, concatenate with $o_{i,t}^{\text{self}}$, and feed actor–critic heads trained by PPO (Schulman et al., 2017).

Reward. To promote goal progress and reciprocal safety (Han et al., 2022), we use $r_t = \alpha(\|p_{i,t} - g_i\| - \|p_{i,t+1} - g_i\|) - \beta \Phi_{\text{RVO}}(\{c_{ij}\}) - \gamma \psi(\min_{j \in \mathcal{N}_i(t)} t_{ij}^{(e)}) - \eta \mathbf{1}\{\text{collision}\}$, where $\alpha, \beta, \gamma, \eta > 0$ are weights; Φ_{RVO} is a smooth, nonnegative VO/RVO penetration measure in velocity space (e.g., sum of hinge distances of $v_{i,t}$ to ORCA half-planes), and $\psi(\cdot)$ penalizes short $t^{(e)}$ (e.g., hinge/reciprocal), both vanishing when constraints are satisfied.

4.3. Deadlock Detection and RL→MAPF Switching Trigger: Purely reactive, decentralized avoidance (e.g., rvo-style reciprocity) is efficient in open space but can stall in tight passages where agents must be *re-ordered* rather than merely sidestepping (van den Berg et al., 2011; Alonso-Mora et al., 2012). This module monitors local kinematics to *detect* such stalemates early and *escalates only a minimal set* of implicated agents to a short, locally confined MAPF subproblem—leaving all others in the RL mode. This on-demand, localized coordination has been shown to reliably resolve doorway/corridor stand-offs while keeping amortized overhead low (Dergachev and Yakovlev, 2021; Dergachev et al., 2020).

Design overview (triggers and roles). We employ three complementary triggers, each targeting a distinct deadlock symptom. (i) *Speed / non-progress* detects *mutual slowing without goal-directed motion* inside a neighborhood—an operational sign of reciprocal stand-off. (ii) *Waypoint-stuck* detects *long-horizon stagnation* by monitoring whether the active waypoint index advances under the global guidance protocol. (iii) *Core-pair risk* identifies an *imminent, reciprocally coupled pair* via short-horizon Time-to-Collision (TTC) / min-distance, which seeds the minimal coordination set. Their *union* yields a fast, low-noise detector that triggers locally confined MAPF only when re-ordering is necessary; non-implicated agents remain in decentralized RL.

Let $p_i(t), v_i(t) \in \mathbb{R}^2$ be the position and velocity of agent i at step t . Denote the active target (current waypoint or final goal) by $w_i^{\text{curr}}(t)$ and the sensed neighbor set $\mathcal{N}_i(t) = \{j \neq i : \|p_j(t) - p_i(t)\| \leq R\}$ with radius R . Define the K -step trailing mean speed $\bar{s}_i(t) = \frac{1}{K} \sum_{\tau=t-K+1}^t \|v_i(\tau)\|$, the unit goal direction $\hat{d}_i(t) = \frac{w_i^{\text{curr}}(t) - p_i(t)}{\|w_i^{\text{curr}}(t) - p_i(t)\|}$ when $\|w_i^{\text{curr}}(t) - p_i(t)\| > \varepsilon_{\text{goal}}$, and the instantaneous progress $\text{prog}_i(t) = \langle v_i(t), \hat{d}_i(t) \rangle$. To avoid spurious triggers we apply gating: $t \geq T_{\text{warm}}$, $\|p_i(t) - w_i^{\text{curr}}(t)\| > \varepsilon_{\text{goal}}$, and $t - t_i^{\text{last}} \geq T_{\text{cool}}$ (where t_i^{last} is the last detection time).

Speed / non-progress trigger. Flag a potential stalemate when an agent moves slowly while at least one neighbor is also slow and not making forward progress:

$$D_{\text{spd}}(i, t) \Leftrightarrow \left(\bar{s}_i(t) < v_{\text{low}} \right) \wedge \left(\exists j \in \mathcal{N}_i(t) : \bar{s}_j(t) < v_{\text{low}} \wedge \text{prog}_j(t) \leq 0 \right), \quad (2)$$

with hyperparameters v_{low} (low-speed threshold) and K (window length).

Waypoint-stuck trigger. If the active waypoint index $k_i(t)$ has not advanced for a budget T_{wp} while the agent remains outside the goal tolerance, raise a deadlock:

$$D_{\text{wp}}(i, t) \Leftrightarrow \left(t - t_i^{\text{wp}}(t) \geq T_{\text{wp}} \right) \wedge \left(\|p_i(t) - w_i^{\text{curr}}(t)\| > \varepsilon_{\text{goal}} \right), \quad (3)$$

where $t_i^{\text{wp}}(t)$ is the last time $k_i(\cdot)$ changed.

Core-pair risk trigger. Using a short-horizon reciprocal-avoidance proxy popular in the literature, including TTC and minimum distance (van den Berg et al., 2011; Alonso-Mora et al., 2012), define

$$r_{ij} = p_j - p_i, \quad u_{ij} = v_j - v_i, \quad \text{ttc}_{ij} = \begin{cases} +\infty, & \|u_{ij}\|^2 \leq \epsilon \text{ or } \langle r_{ij}, u_{ij} \rangle \geq 0 \\ -\frac{\langle r_{ij}, u_{ij} \rangle}{\|u_{ij}\|^2}, & \text{otherwise} \end{cases},$$

and $d_{\min_{ij}} = \|r_{ij}\|$ if $\text{ttc}_{ij} = +\infty$, else $d_{\min_{ij}} = \|r_{ij} + \text{ttc}_{ij} u_{ij}\|$. Let $b(i) = \arg \min_{j \in \mathcal{N}_i(t)} \text{ttc}_{ij}$ (ties broken deterministically). A mutually “most-at-risk” pair with imminent interaction activates:

$$D_{\text{risk}}(i, t) \Leftrightarrow \left(b(b(i)) = i \right) \wedge \left(\text{ttc}_{i b(i)} < \tau_{\text{ttc}} \vee d_{\min_{i b(i)}} < \delta_{\min} \right), \quad (4)$$

with thresholds τ_{ttc} and δ_{\min} (and small ϵ for numerical stability).

Union rule and switch logic. A deadlock is declared for agent i whenever any trigger fires: $D(i, t) = D_{\text{spd}}(i, t) \vee D_{\text{wp}}(i, t) \vee D_{\text{risk}}(i, t)$, subject to the gating above. From the seed agent, we form a *minimal* participant set by (i) including the core pair when (4) holds and (ii) applying a tiny consensus closure within $\mathcal{N}_i(t)$ to cover the immediate stalemate. The selected set is *locked* for T_{lock} steps to prevent oscillations; only agents for which a valid locally confined MAPF subplan is found switch to the MAPF mode, and all others remain in decentralized RL. This localized, on-demand escalation mirrors prior “locally confined MAPF” hybrids that resolve doorway/corridor stand-offs without team-wide coordination.

4.4. Local MAPF Instance: The triggers in §4.3 produce a *local, minimal* set of implicated agents and a detection time t . This subsection turns that signal into a concrete coordination problem by (i) freezing the participant set and identifying the *coordination group*, (ii) cropping a subgrid \mathcal{G}' around them, (iii) instantiating a *locally confined MAPF* $\mathcal{I}' = \langle \mathcal{G}', \mathcal{A}_{\text{lc}}, S, T \rangle$ using current poses as starts and projected active waypoints as local goals, and (iv) solving \mathcal{I}' quickly to obtain per-agent *dense waypoint lists*. These lists are executed by the *same decentralized RL policy* (others remain in RL), and once the dense segments finish, all agents revert to tracking their original global waypoints. This “detect→crop→coordinate→handover” design follows prior locally confined MAPF frameworks for doorway/corridor stand-offs and uses PnR for fast, complete reordering on the subgrid. Upon a deadlock trigger, a set of nearby agents enters a locally confined coordination phase on a subgrid \mathcal{G}' .

For the deadlock-triggering agent i at time t , we define the local neighbor set within sensing radius R as $\mathcal{N}_i(t) = \{j \in \mathcal{A} \setminus \{i\} \mid \|p_j(t) - p_i(t)\|_2 \leq R\}$, $\mathcal{A}_{lc}(t) = \{i\} \cup \mathcal{N}_i(t)$. Here, \mathcal{A} is the finite index set of agents; $p_i(t) \in \mathbb{R}^2$ denotes the position of agent i at discrete step $t \in \mathbb{N}$; $R > 0$ is the sensing radius; and $\|\cdot\|_2$ is the Euclidean norm.

All the other agents remain in decentralized RL mode. We construct \mathcal{G}' by padding the participants' axis-aligned bounding box with margin $m > 0$ and discretizing at resolution h_g . Starts $S(\cdot)$ are assigned by nearest-cell projection of current poses; local goals $T(\cdot)$ are obtained by projecting each agent's active global waypoint into \mathcal{G}' .

Solver and execution. We solve the local MAPF instance $\mathcal{I}' = \langle \mathcal{G}' = (V', E'), \mathcal{A}_{lc}, S, T \rangle$ with *Push-and-Rotate (PnR)* algorithm (de Wilde et al., 2014). The joint discrete plan for each participant is converted into a short *dense waypoint list* (time-ordered references) and tracked by the *same* RL low-level controller under a mild speed cap; non-participants continue with RL. After the dense lists are executed (stalemate cleared), agents revert to the default RL navigator and resume tracking their original global waypoint lists. Full pseudo-code for PnR on the cropped subgrid, along with the completeness condition (two blanks per component) and the polynomial-time bound, are provided in Appendix A.

4.5. Formal Guarantees for Triggered RL+MAPF Coordination: We give formal guarantees for the *trigger \rightarrow locally confined MAPF \rightarrow execution* cycle on the cropped subgrid \mathcal{G}' , as used by the Hybrid method. Let $\mathcal{A}_{lc}(t)$ be the participant set at trigger time t , and let $\mathcal{I}' = \langle \mathcal{G}', \mathcal{A}_{lc}, S, T \rangle$ be the induced local MAPF instance; S projects current poses to V' , and T projects the *active global waypoints* to V' . PnR primitives, invariants, and theorems are stated in Appendix A. Let Π be the collision-free joint discrete plan returned by PnR on \mathcal{G}' with horizon L . For each $a \in \mathcal{A}_{lc}$, build a dense waypoint list $\mathcal{W}_a^{\text{dense}}$ by projecting the vertices of Π to world-frame cell centers and collapsing consecutive waits. During execution, the same decentralized RL policy tracks $\mathcal{W}_a^{\text{dense}}$ under the standard speed bound.

Theorem 1 (Finite-step deadlock clearance) *Assume that every connected component C of \mathcal{G}' contains at least two blanks ($b(C) \geq 2$) and that the induced instance \mathcal{I}' is solvable. Then PnR returns Π ; moreover, after tracking $\{\mathcal{W}_a^{\text{dense}}\}$, every $a \in \mathcal{A}_{lc}$ increases its active global waypoint index by at least one in a finite number of simulator steps. Hence the local stalemate is cleared and long-range progress resumes for all participants.*

Proof By Appendix A, Theorem 4, PnR is complete on \mathcal{G}' under $b(C) \geq 2$ and returns a collision-free plan Π whenever \mathcal{I}' is solvable (cf. de Wilde et al., 2014). By construction (§.4.4), each local target $T[a]$ is the grid projection of a 's *active global waypoint* region. Mapping Π to $\mathcal{W}_a^{\text{dense}}$ preserves vertex order and yields a finite sequence. The decentralized RL tracker advances along $\mathcal{W}_a^{\text{dense}}$ and enters the cell of $T[a]$ within finitely many simulator ticks (bounded speed and cell diameter). The waypoint manager then increments the active waypoint index for a . Since this holds for every $a \in \mathcal{A}_{lc}$, the stalemate is cleared for the whole group. ■

Theorem 2 (Polynomially bounded coordination overhead) *Under the same precondition $b(C) \geq 2$, the number of primitive operations emitted by PnR on \mathcal{G}' is polynomial in $|V'|$ and $|\mathcal{A}_{lc}|$ (Appendix A, Theorem 5). Consequently, the plan horizon L and the total dense-waypoint length $\sum_{a \in \mathcal{A}_{lc}} |\mathcal{W}_a^{\text{dense}}|$ are $O(\text{poly}(|V'|, |\mathcal{A}_{lc}|))$, implying that the per-trigger duty cycle (fraction of execution steps under coordination) is polynomially bounded by crop size and group size.*

Proof Appendix A, Theorem 5 states that PnR runs in polynomial time and emits a polynomial number of primitive operations in $|V'|$ and $|\mathcal{A}_{lc}|$ (cf. de Wilde et al., 2014). Each primitive contributes $O(1)$ appended vertices per agent when forming Π , thus $L = O(\text{poly}(\cdot))$. The mapping $\Pi \mapsto \{\mathcal{W}_a^{\text{dense}}\}$ collapses waits and never expands steps, so $\sum_a |\mathcal{W}_a^{\text{dense}}| = O(L)$. Execution consumes at most a constant number of simulator ticks per dense waypoint (bounded speed, bounded cell diameter), hence the duty cycle per trigger is polynomially bounded as claimed. ■

Context. Our “trigger → locally confined MAPF → handover” construction follows the locally confined MAPF design for resolving doorway/corridor stand-offs (e.g., Dergachev and Yakovlev, 2021) and uses PnR for fast, complete reordering on the crop while all non-participants remain in decentralized RL.

5. Experiment

5.1. Simulation Setup: We evaluate in two static 2D maps that stress long-range progress under geometric bottlenecks: a **doorway** (short bottleneck) and a **corridor** (long single-lane) scenario, both known to induce reciprocal stand-offs for purely reactive VO style controllers (Han et al., 2022; Fiorini and Shiller, 1998; van den Berg et al., 2011; Stern et al., 2019a). Robots are discs moving in discrete time with kinematics and sensing as in Problem Formulation; all core simulator parameters are summarized in Appendix B.

For long-range guidance we use A* algorithm to generate per-agent global waypoint lists on a grid aligned with the world frame. Local navigation is *always* executed by the same trained RL policy (RL-RVO style features and shaping), which tracks either global waypoints (default) or dense temporary waypoints returned by the local MAPF when triggered. We compare **RL-only** vs. **RL+MAPF (ours)** under identical policies and maps to isolate the effect of the triggered local coordination. All the training and evaluations are conducted on a single workstation with CPU Intel Core i9-13900KF and GPU NVIDIA GeForce RTX 4080. The RL policy is trained by using PPO as the on-policy optimizer (Schulman et al., 2017); other training details follow Han et al. (2022).

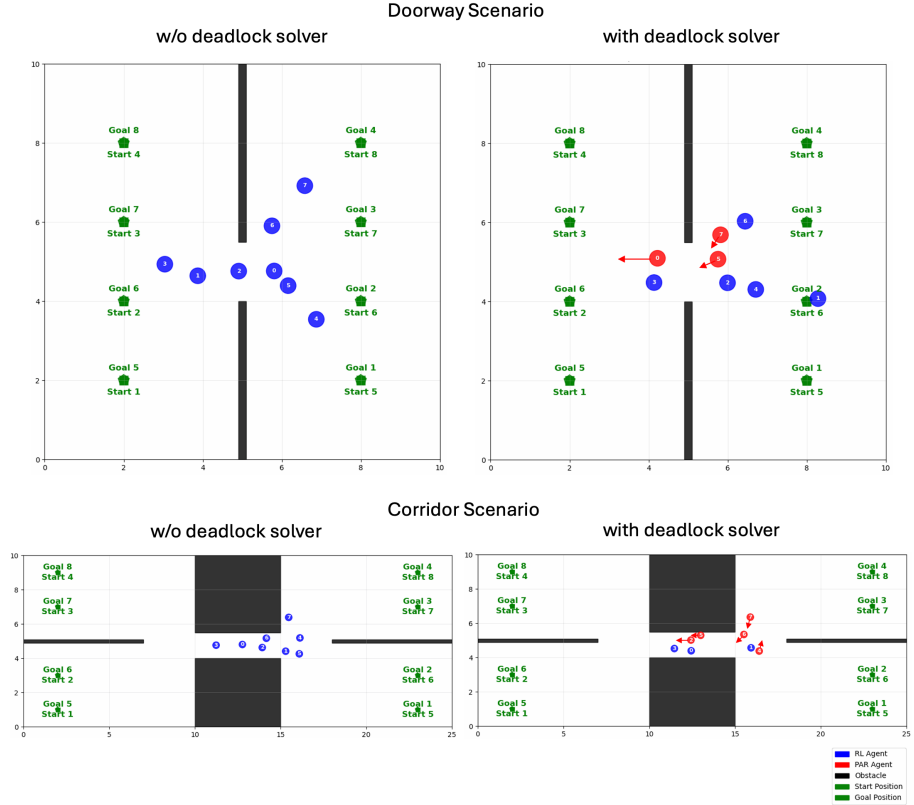
5.2. Methods Under Comparison: Our goal is *not* to rank different local navigation models. Instead, we propose a **hybrid wrapper**—deadlock detection + locally confined MAPF—that can be applied to an existing local navigator with minimal changes. Accordingly, we hold the base RL navigator fixed and compare it *with vs. without* the wrapper to isolate the incremental effect of local coordination, in line with prior locally confined hybrids (Dergachev and Yakovlev, 2021). We conducted the comparison as:

- **RL-only (Base).** The decentralized RL local navigator runs alone (no deadlock detector, no MAPF), following Han et al. (2022).
- **Hybrid (Ours).** The *same* RL navigator augmented with: (i) the deadlock detector; and (ii) a locally confined MAPF module that solves the cropped subproblem with **Push-and-Rotate (PnR)** (de Wilde et al., 2014).

5.3. Evaluation Protocol & Metrics: For each scenario (doorway, corridor), each agent count/density, and each method (RL-only vs. Hybrid), we run $N = 100$ independent episodes and report aggregated results. An episode is declared *timeout* if any agent has not reached its goal within $T_{\text{max}} = 1000$ simulation steps. An episode is a *success* iff *all* agents reach their goals within

Table 1: Success rate (%) over $N=100$ trials per setting.

Method	Doorway			Corridor		
	4	6	8	4	6	8
RL-only	15.63%	47.95%	39.34%	8.82%	0.00%	0.00%
Hybrid (PnR)	100.00%	98.44%	95.45%	100.00%	100.00%	100.00%

Figure 3: Qualitative comparison in **Doorway** (left two panels) and **Corridor** (right two panels).

T_{\max} with no collisions. To ensure fairness, all methods share identical environment and protocol. The primary metric is *success rate*, standard for MAPF/navigation evaluations where reaching all goals is the main objective. We do not claim improvements in average time/path length across all settings; local coordination can introduce bounded waiting or detours by design.

5.4. Result Analysis (Doorway Scenario): We use a single short bottleneck with doorway width 1.5 m. Agent counts are $\{4, 6, 8\}$. Starts/goals are *fixed and symmetric* (left starts are right goals and vice versa). For each agent count and each method (RL-only vs. Hybrid), we run $N=100$ episodes with timeout $T_{\max}=1000$ steps and declare success only if *all* agents reach goals. Table 1 reports the success rate. Hybrid (RL + deadlock trigger + local PnR) consistently improves completion in this short-bottleneck setting. Figure 3 (left panels) visualizes the effect: RL-only (left-most) settles into a reciprocal “yield–stall” in front of the doorway, whereas with the deadlock solver (second panel) a small red subset is temporarily coordinated to pass, restoring two-way flow while non-participants

remain in RL. In short bottlenecks, *minimal* coordination suffices to unlock progress, aligning with our on-demand local MAPF design.

5.5. Result Analysis (Corridor Scenario): We evaluate a long single-lane corridor of length 5 m and width 1.5 m with two-way traffic. Agent counts are $\{4, 6, 8\}$ with the same fixed symmetric starts/goals. We use the same protocol as the doorway case: $N=100$, $T_{\max}=1000$, success iff all agents reach goals. Table 1 summarizes the rates: RL-only degrades sharply with density, while the Hybrid maintains high completion via occasional PnR interventions. Figure 3 (right panels) shows why: the long bottleneck induces a persistent impasse under RL-only (third panel), but the triggered local MAPF (fourth panel, red subset) produces a feasible passing order inside the cropped subgrid and clears the stalemate; the rest of the team continues under decentralized RL. This matches our goal: invoke coordination only where/when re-ordering is necessary, leaving the remainder to RL.

6. Conclusions

We proposed a hybrid, model-agnostic navigation framework that integrates decentralized RL with on-demand, locally bounded MAPF to resolve topological deadlocks. The wrapper intervenes only when progress stalls, applying Push-and-Rotate on a cropped subregion before returning control to RL. In doorway and corridor scenarios, the method consistently turned stalled interactions into successful completions while keeping coordination local. Future work includes adaptive deadlock detection, dynamic subregion sizing, and solver selection to further balance success and efficiency.

References

Javier Alonso-Mora, Andreas Breitenmoser, Paul Beardsley, and Roland Siegwart. Reciprocal collision avoidance for multiple car-like robots. In *IEEE International Conference on Robotics and Automation (ICRA)*, pages 360–366, 2012.

Anton Andreychuk, Konstantin S. Yakovlev, Dor Atzmon, and Roni Stern. Multi-agent pathfinding with continuous time. *Artificial Intelligence*, 305:103664, 2022.

Dor Atzmon, Ariel Felner, Roni Stern, Glenn Wagner, and Roman Bart’ak. Multi-agent path finding for large teams: The increasing cost of optimality. In *AAAI Conference on Artificial Intelligence*, pages 7207–7214, 2020.

Max Barer, Guni Sharon, Roni Stern, and Ariel Felner. Suboptimal variants of the conflict-based search algorithm for the multi-agent pathfinding problem. In *Symposium on Combinatorial Search (SoCS)*, pages 19–27, 2014.

Eli Boyarski, Ariel Felner, Roni Stern, Guni Sharon, David Tolpin, Oded Betzalel, and Solomon Eyal Shimony. ICBS: Improved conflict-based search algorithm for multi-agent pathfinding. In *Proceedings of the 24th International Joint Conference on Artificial Intelligence (IJCAI)*, pages 740–746, 2015.

Hoang-Dung Bui. A survey of multi-robot motion planning. *arXiv preprint arXiv:2310.08599*, 2023.

Mingyu Cai, Erfan Aasi, Calin Belta, and Cristian-Ioan Vasile. Overcoming exploration: Deep reinforcement learning for continuous control in cluttered environments from temporal logic specifications. *IEEE Robotics and Automation Letters*, 8(4):2158–2165, 2023.

Changan Chen, Yuejiang Liu, Sven Kreiss, and Alexandre Alahi. Crowd-robot interaction: Crowd-aware robot navigation with attention-based deep reinforcement learning. In *IEEE International Conference on Robotics and Automation (ICRA)*, pages 6015–6022, 2019.

Yunzhu Chen, Mingyang Liu, Michael Everett, and Jonathan P. How. Decentralized non-communicating multiagent collision avoidance with deep reinforcement learning. In *IEEE International Conference on Robotics and Automation (ICRA)*, pages 285–292, 2017.

Boris de Wilde, Adriaan W. ter Mors, and Cees Witteveen. Push and rotate: cooperative multi-agent path planning. In *Proceedings of the 2013 International Conference on Autonomous Agents and Multi-Agent Systems*, 2013.

Brent de Wilde, Adriaan W. ter Mors, and Cees Witteveen. Push and rotate: a complete multi-agent pathfinding algorithm. *Journal of Artificial Intelligence Research*, 51:443–492, 2014.

Stepan Dergachev and Konstantin Yakovlev. Distributed multi-agent navigation based on reciprocal collision avoidance and locally confined multi-agent path finding. *arXiv preprint arXiv:2107.00246*, 2021.

Stepan Dergachev, Konstantin Yakovlev, and Ryhor Prakapovich. A combination of theta*, orca and push and rotate for multi-agent navigation. In *International Conference on Interactive Collaborative Robotics (ICR)*, volume 12336 of *Lecture Notes in Computer Science*, pages 55–66, 2020.

Michael Everett, Yunzhu Chen, and Jonathan P. How. Ga3c-cadrl: Collision avoidance with deep reinforcement learning. In *IEEE/RSJ International Conference on Intelligent Robots and Systems (IROS)*, pages 667–673, 2018.

Tingxiang Fan, Pinxin Long, Wenxi Liu, and Jia Pan. Distributed multi-robot collision avoidance via deep reinforcement learning for navigation in complex scenarios. *The International Journal of Robotics Research*, 39(7):856–892, 2020. doi: 10.1177/0278364920916531.

Paolo Fiorini and Zvi Shiller. Motion planning in dynamic environments using velocity obstacles. *The International Journal of Robotics Research*, 17(7):760–772, 1998.

David Ge, Hao Ji, and Bingling Huang. Efficient training in multi-agent reinforcement learning: A communication-free framework for the box-pushing problem. In *International Design Engineering Technical Conferences and Computers and Information in Engineering Conference*, volume 89213, page V02BT02A039. American Society of Mechanical Engineers, 2025.

Jaskaran Grover, Changliu Liu, and Katia Sycara. Deadlock analysis and resolution in multi-robot systems (extended version). *arXiv preprint arXiv:1911.09146*, 2019. URL <https://arxiv.org/abs/1911.09146>. Formal characterization of deadlock for CBF-based multi-robot controllers and a decentralized resolution algorithm.

Stephen J. Guy, Jatin Chhugani, Changkyu Kim, Nadathur Satish, Ming C. Lin, Dinesh Manocha, and Pradeep Dubey. ClearPath: Highly parallel collision avoidance for multi-agent simulation. In *Proceedings of the ACM SIGGRAPH/Eurographics Symposium on Computer Animation (SCA)*, pages 177–187, New Orleans, LA, USA, August 2009. ACM. doi: 10.1145/1599470.1599494.

Ruihua Han, Shengduo Chen, Shuaijun Wang, Zeqing Zhang, Rui Gao, Qi Hao, and Jia Pan. Reinforcement learned distributed multi-robot navigation with reciprocal velocity obstacle shaped rewards. *arXiv preprint arXiv:2203.10229*, 2022.

Peter E. Hart, Nils J. Nilsson, and Bertram Raphael. A formal basis for the heuristic determination of minimum cost paths. *IEEE Transactions on Systems Science and Cybernetics*, SSC-4(2):100–107, 1968. doi: 10.1109/TSSC.1968.300136.

Bingling Huang, Hao Ji, and Yan Jin. Impact of social learning on teamwork efficiency in learning-based self-organized systems. In *International Design Engineering Technical Conferences and Computers and Information in Engineering Conference*, volume 88377, page V03BT03A002. American Society of Mechanical Engineers, 2024.

Jiaoyang Li, Zhe Chen, Daniel Harabor, Peter J. Stuckey, and Sven Koenig. Anytime multi-agent path finding via large neighborhood search. In *Proceedings of the 30th International Joint Conference on Artificial Intelligence (IJCAI)*, pages 4115–4123, 2021a. doi: 10.24963/ijcai.2021/568.

Jiaoyang Li, Daniel Harabor, Peter J. Stuckey, and Sven Koenig. Anytime and bounded-suboptimal multi-agent path finding via enhanced conflict-based search. In *AAAI Conference on Artificial Intelligence*, pages 12353–12361, 2021b.

Jiaoyang Li, Wheeler Ruml, and Sven Koenig. Mapf-lns: Large neighborhood search for multi-agent path finding. In *International Joint Conference on Artificial Intelligence (IJCAI)*, pages 4127–4135, 2021c.

Pinxin Long, Tingxiang Fan, Xinyi Liao, Wenxi Liu, Hao Zhang, and Jia Pan. Towards optimally decentralized multi-robot collision avoidance via deep reinforcement learning. In *Proceedings of the IEEE International Conference on Robotics and Automation (ICRA)*, pages 6252–6259, Brisbane, Australia, 2018. IEEE. doi: 10.1109/ICRA.2018.8461113.

Ryan Luna and Kostas E. Bekris. Push and swap: fast cooperative path-finding with completeness guarantees. *IJCAI’11*, 2011.

Licheng Luo and Mingyu Cai. Bridging deep reinforcement learning and motion planning for model-free navigation in cluttered environments. *arXiv preprint arXiv:2504.07283*, 2025.

Hang Ma, Alex Tinka, Casey Kumar, Nora Ayanian, and Sven Koenig. Lifelong multi-agent path finding in large-scale warehouses. In *AAAI Conference on Artificial Intelligence*, pages 11272–11281, 2021.

Alex Nash, Sven Koenig, Craig Tovey, and Ariel Felner. Theta*: Any-angle path planning on grids. In *AAAI Conference on Artificial Intelligence*, pages 1177–1183, 2007.

Alex Nash, Sven Koenig, Maxim Likhachev, Craig A. Tovey, and Ariel Felner. Lazy theta*: Any-angle path planning and path length analysis in 3d. In *AAAI Conference on Artificial Intelligence*, pages 147–154, 2010.

John Schulman, Filip Wolski, Prafulla Dhariwal, Alec Radford, and Oleg Klimov. Proximal policy optimization algorithms. *arXiv preprint arXiv:1707.06347*, 2017.

Guni Sharon, Roni Stern, Ariel Felner, and Nathan R. Sturtevant. Conflict-based search for optimal multi-agent pathfinding. *Artificial Intelligence*, 219:40–66, 2015.

Jamie Snape, Jur van den Berg, Stephen J. Guy, and Dinesh Manocha. The hybrid reciprocal velocity obstacle. *IEEE Transactions on Robotics*, 27(4):696–706, 2011.

Roni Stern, Nathan R. Sturtevant, Ariel Felner, Sven Koenig, Hang Ma, Thayne Walker, Jiaoyang Li, Dor Atzmon, Liron Cohen, T. K. Satish Kumar, Eli Boyarski, and Roman Barták. Multi-agent pathfinding: Definitions, variants, and benchmarks. *Proceedings of the International Symposium on Combinatorial Search (SoCS)*, pages 151–158, 2019a.

Roni Stern, Nathan R. Sturtevant, Ariel Felner, Sven Koenig, Hang Ma, Thayne T. Walker, Jiaoyang Li, Dor Atzmon, Liron Cohen, T. K. Satish Kumar, Eli Boyarski, and Roman Barták. Multi-agent pathfinding: Definitions, variants, and benchmarks. In *Proceedings of the 12th International Symposium on Combinatorial Search (SoCS)*, pages 151–158, 2019b.

Pavel Surynek, Roni Stern, Ariel Felner, T. K. Satish Kumar, and Sven Koenig. Multi-agent path finding with generalized conflict-based search. *IEEE Robotics and Automation Letters*, 6(3):4495–4502, 2021.

Jur van den Berg, Stephen J. Guy, Ming C. Lin, and Dinesh Manocha. Reciprocal n-body collision avoidance. *The International Journal of Robotics Research*, 27(7):1071–1087, 2011.

Ko-Hsun Chen Wang and Adi Botea. Fast and memory-efficient multi-agent pathfinding. In *Proceedings of the 18th International Conference on Automated Planning and Scheduling (ICAPS)*, pages 380–387, 2008. URL <https://cdn.aaai.org/ICAPS/2008/ICAPS08-047.pdf>. Defines execution deadlocks as cycles of agents waiting for each other and proposes a heuristic breaking procedure.

Konstantin Yakovlev and Anton Andreychuk. Any-angle pathfinding for multiple agents based on sipp algorithm. In *International Conference on Automated Planning and Scheduling (ICAPS)*, pages 586–593, 2017.

Appendix A. Locally Confined Push-and-Rotate (PnR) on a Cropped Subgrid

This appendix formalizes the primitives and guarantees of the *locally confined* Push-and-Rotate (PnR) procedure used by our deadlock solver. PnR is complete on graphs whose every connected component has at least two unoccupied vertices (“blanks”) and admits polynomial running time bounds (de Wilde et al., 2014, 2013). We restate the setting on the cropped subgrid \mathcal{G}' and then give formal definitions for the primitives (*push*, *swap*, *rotate*) followed by complete proofs of the two theorems.

A.1. Problem restatement on the cropped subgrid

Given a cropped subgrid $\mathcal{G}' = (V', E')$ around the implicated agents \mathcal{A}_{lc} , we define a local MAPF instance $\mathcal{I}' = \langle \mathcal{G}', \mathcal{A}_{lc}, S, T \rangle$, where $S : \mathcal{A}_{lc} \rightarrow V'$ and $T : \mathcal{A}_{lc} \rightarrow V'$ are the start and (local) target assignments obtained by projecting current poses and active global waypoints into \mathcal{G}' . Time is discretized by unit steps; at most one agent occupies a vertex at any time; moves are to adjacent vertices or a wait action.

A (partial) configuration is a function $A : V' \rightarrow \mathcal{A}_{lc} \cup \{\perp\}$, where $A(v) = \perp$ denotes a blank. For a connected component C of \mathcal{G}' , let $b(C) := |\{v \in C : A(v) = \perp\}|$ be its blank count. We maintain a set $F \subseteq \mathcal{A}_{lc}$ of *finished* agents frozen at their targets.

A.2. PnR primitives: formal definitions

We write $A \Rightarrow A'$ for a single discrete-time transition of the configuration (possibly moving multiple non-conflicting agents simultaneously). Below, $P = (v_0, \dots, v_k)$ denotes a simple path in \mathcal{G}' .

Push. Let $r \in \mathcal{A}_{lc} \setminus F$ be the active agent and $P = (v_0, \dots, v_k)$ a shortest path from $A^{-1}(r) = v_0$ to $T[r]$ in $\mathcal{G}' \setminus A[F]$. Suppose the next vertex v_1 is occupied by a *blocker* $b \notin F$ and there exists a simple path $Q = (u_0, \dots, u_\ell)$ inside the same connected component C with $u_0 = v_1$, u_ℓ blank, and all u_j distinct such that $b(C) \geq 2$ holds throughout.¹ A *push* of b along Q is the sequence of transitions that shifts the blank from u_ℓ back to $u_0 = v_1$:

$$A(u_j) = \begin{cases} \perp & j = \ell \\ x_{j+1} & 0 \leq j < \ell \end{cases} \quad \rightsquigarrow \quad A'(u_j) = \begin{cases} x_j & 1 \leq j \leq \ell \\ \perp & j = 0 \end{cases}$$

where $x_j = A(u_j)$ are the pre-push occupants. After the push, v_1 becomes blank, enabling r to advance to v_1 on the next step. No vertex in $A[F]$ is modified.

Swap (within a biconnected block). Let u, v be adjacent vertices in the same biconnected component (block) $B \subseteq C$ with $A(u) = r$, $A(v) = b \notin F$, and $b(B) \geq 1$ (there exists a blank elsewhere in B). A *swap* is a constant-size sequence of moves inside B that exchanges the positions of r and b while leaving all other agents unchanged and preserving $b(C) \geq 2$. Existence follows from the presence of a cycle in B and one blank, allowing a 3–4 move exchange on a simple cycle (standard 15-puzzle–style maneuver) (Luna and Bekris, 2011).

Rotate (on a simple cycle). Let $Z = (z_0, \dots, z_{k-1}, z_k = z_0)$ be a simple cycle in a component C with at least one blank on Z . A *rotate* moves each agent on Z to the next vertex along the cycle in the same direction, filling the blank; since C has $b(C) \geq 2$, at least one blank remains off-cycle, preserving the two-blank invariant. Rotation never touches $A[F]$ and keeps agents inside the same block (de Wilde et al., 2014).

A.3. Algorithmic scheme

We instantiate PnR on \mathcal{G}' as in Alg. 1: route one active agent along a shortest path that avoids finished agents; when encountering conflicts, resolve them by *push/swap/rotate*. The joint plan Π is later converted into a short *dense waypoint list* for each participant and tracked by the same RL low-level controller.

1. If needed, a short *clear* step is taken to create a temporary blank away from $A[F]$, as in de Wilde et al. (2014).

Algorithm 1: Locally confined Push-and-Rotate (PnR) on cropped subgrid **Fix the Alg.** \mathcal{G}'

Input : $\mathcal{G}' = (V', E')$; participants \mathcal{A}_{lc} ; starts S ; targets T

Output: Joint collision-free discrete plan Π over \mathcal{G}'

```

1  $A \leftarrow S$            // current assignment (at most one agent per vertex)
2  $F \leftarrow \emptyset$       // finished set (agents fixed at targets)
3 while  $F \neq \mathcal{A}_{lc}$  do
4   Choose  $r \in \mathcal{A}_{lc} \setminus F$  (e.g., by ID or heuristic) Compute a shortest path  $p$  from  $A^{-1}(r)$  to  $T[r]$ 
   in  $\mathcal{G}' \setminus A[F]$  while  $A^{-1}(r) \neq T[r]$  do
7      $u \leftarrow$  next vertex on  $p$  if  $u$  is blank then
6       move  $r \rightarrow u$ ; append to  $\Pi$ ; update  $A$ 
7     else if  $p$  closes a simple cycle in the current block then
8       ROTATE along that cycle; append moves; update  $A$ 
9     else if there exists a blocker  $b \notin F$  at  $u$  then
10      PUSH  $b$  to a nearby blank (preserving two blanks per component and avoiding  $A[F]$ );
           append moves; update  $A$ 
11    else
12      SWAP  $r$  with an adjacent blocker in the same block; append moves; update  $A$ 
13    end
14  end
15   $F \leftarrow F \cup \{r\}$            // freeze  $r$  at  $T[r]$ 
16 end
17 return  $\Pi$ 

```

A.4. Invariants and potential function

We maintain the following invariants at every step:

- (I1) **Finished fixed:** $A[F] = T[F]$ and finished vertices are never modified.
- (I2) **Two blanks per component:** $b(C) \geq 2$ for every connected component C .
- (I3) **Active simple path:** for the active agent r , there exists a simple path p_r from $A^{-1}(r)$ to $T[r]$ in $\mathcal{G}' \setminus A[F]$.

Define the lexicographic potential

$$\Phi(A, r) = (D_r(A), K_r(A), H_r(A)) \in \mathbb{N}^3,$$

where (i) D_r is the graph distance from $A^{-1}(r)$ to $T[r]$ in $\mathcal{G}' \setminus A[F]$, (ii) K_r is the number of non-finished blockers present on the chosen shortest path p_r , and (iii) H_r is the sum of shortest-path distances from each blocker on p_r to the nearest blank within its component (computed in $\mathcal{G}' \setminus A[F]$). We order potentials lexicographically, i.e., $(a, b, c) \prec (a', b', c')$ iff $a < a'$ or $(a = a'$ and $b < b'$) or $(a = a', b = b'$ and $c < c'$).

Lemma 3 (Local progress) *Under invariants (I1)–(I3), any of the primitives (push, swap, rotate) preserves (I1)–(I3) and yields $\Phi(A', r) \prec \Phi(A, r)$, where $A \Rightarrow A'$ is the resulting configuration (and r remains the active agent unless it moves to its target).*

Proof (I1) holds since primitives explicitly avoid $A[F]$. (I2) holds because each primitive either moves an existing blank within a component (push), uses a cycle with at least one off-cycle blank guaranteed by $b(C) \geq 2$ (rotate), or executes a constant-size exchange within a biconnected block without consuming blanks (swap) (de Wilde et al., 2014; Luna and Bekris, 2011). For Φ : a blank delivered to the next vertex on p_r either lets r advance one step (D_r strictly decreases), or reduces the count of blockers K_r ; when neither applies, the relocation of a blocker strictly reduces its distance to a blank, decreasing H_r . Rotation on a cycle containing a blocker advances the blank past that blocker, decreasing K_r or H_r . Swap decreases K_r directly by exchanging r with the front blocker. Thus Φ strictly decreases in lexicographic order. \blacksquare

A.5. Main guarantees

Theorem 4 (Completeness with two blanks per component) *Let \mathcal{G}' be any graph in which every connected component C has at least two blanks, i.e., $b(C) \geq 2$ for all C . Then for any solvable instance $\mathcal{I}' = \langle \mathcal{G}', \mathcal{A}_{lc}, S, T \rangle$, PnR returns a collision-free plan Π that solves \mathcal{I}' .*

Proof Initiate with $F = \emptyset$ and pick any $r \in \mathcal{A}_{lc} \setminus F$. By solvability and (I2), a path p_r exists in $\mathcal{G}' \setminus A[F]$, so (I3) holds. By Lemma 3, every primitive preserves invariants and strictly decreases $\Phi(A, r)$ until either (a) r reaches $T[r]$ or (b) another agent becomes the active agent with smaller D_r at its turn; in both cases, termination occurs in finitely many steps because $\Phi \in \mathbb{N}^3$ is well-founded. When r reaches $T[r]$, we freeze it: $F \leftarrow F \cup \{r\}$, which preserves (I1)–(I2). Repeating this process assigns all agents to $T[\cdot]$ in finitely many phases (at most $|\mathcal{A}_{lc}|$). Since primitives never modify finished vertices and moves are adjacent or wait, the concatenation yields a collision-free plan. Hence PnR returns a valid solution whenever one exists. \blacksquare

Theorem 5 (Polynomial running time) *Under the same precondition $b(C) \geq 2$ for all components C of \mathcal{G}' , PnR runs in time polynomial in $|V'|$ and $|\mathcal{A}_{lc}|$.*

Proof As shown by de Wilde et al. (2014), each agent becomes active a bounded number of phases and, in each phase, the number of primitive operations (push/swap/rotate) is bounded by a polynomial in $|V'|$ (each operation affects a constant-size pattern, and path recomputations can be done in $O(|E'|)$ time). Summing over at most $|\mathcal{A}_{lc}|$ agents yields a polynomial bound on the total number of operations and the running time in $|V'|$ and $|\mathcal{A}_{lc}|$. Therefore, PnR admits a polynomial-time complexity on \mathcal{G}' . \blacksquare

A.6. From discrete plan to execution

The joint plan Π is converted into a short *dense waypoint list* for each participant. During execution, the same decentralized RL policy tracks these dense waypoints while handling reciprocal avoidance; upon completion, agents revert to the default RL navigation and resume their original global waypoint lists.

Appendix B. Simulator Parameters

Table 2: Core simulator parameters used in all experiments.

Parameter	Symbol	Value
Time step	Δt	0.1 s
Control frequency	f_c	10 Hz
Max speed	v_{\max}	1.5 m/s
Agent radius	r	0.2 m
Sensing horizon	R	5 m
Neighbor cap (impl.)	n/a	10